Article ID: 1006-8775(2019) 03-0304-08

REFINED RISK ASSESSMENT OF STORM SURGE DISASTER IN COASTAL PLAIN: A CASE STUDY OF PINGYANG COUNTY

CHEN Fu-yuan (陈甫源), YU Pu-bing (于普兵), WU Xiu-guang (吴修广), ZHU Yun-ze (朱韫泽)
(Key Laboratory of Estuary and Coast of Zhejiang Province, Zhejiang Institute of Hydraulics and Estuary, Hangzhou 310020 China)

Abstract: As the risk of storm surge on coastal plains increases, the research on disaster risk assessment is fundamental for disaster management. Disaster risk assessment tends to develop towards the direction of refinement and it gradually plays a more important role. According to the characteristics of storm surge disaster in coastal plain, the paper uses refined floodplain numerical model which combines typhoon, flood, astronomical tide and waves to simulate inundation process. The model also considers influencing factors of dike-breaking, micro-topography and buildings. Precise calculation is executed for the range and the submerged depth caused by floodplain flow in coastal plain. Based on 3S technology, disaster-bearing bodies are subdivided into the smallest unit of the ground object, and the vulnerability of these units is evaluated. Refined risk assessment of storm surge disaster for the coastal plain is obtained, and the detailed distribution of risk areas at different risk levels is achieved. These results can be widely applied in many fields, such as disaster prevention and mitigation, urban planning, industrial arrangement, disaster insurance and so on.

Key words: coastal plain; storm surge; submergence; risk assessment
CLC number: P732 **Document code:** A
doi: 10.16555/j.1006-8775.2019.03.002

1 INTRODUCTION

In China, coastal plains are mainly located in both sides of the estuary. They are not only the economic and population gathering areas, but also the main carriers of society development for the past several decades. Because terrain is low and flat, coastal plains are jointly influenced by storm surge, astronomical tide and basin flood in typhoon weather. This situation is very likely to cause serious inundation and huge economic loss (Wang et al.[1]). For example, Yuyao is a small city of Zhejiang province and 70% of its area was so seriously inundated during the typhoon "Fitow" (2013) that an insurance company had to pay for the damage three times as much as its profits accumulated over the past 60 years (Gu et al.[2]). Recently, as global warming intensifies and sea level rises (Wang et al.[3]), extreme weather events occur more frequently than before (Yin et al.[4]; Li et al.[5]). It is urgent to improve the technical support capacity of disaster prevention and mitigation. As the core of disaster prevention and mitigation, pre-disaster management is the most important part and risk assessment is the basic work. Risk assessment is widely used in the design of pre-disaster prevention, rescue in disaster and post-disaster reconstruction. It is also used in urban planning, industry layout optimization, disaster insurance, and so on. As early as 1980s and 1990s, western countries, e.g., the United States, carried out a systematical risk assessment of coastal storm surge disaster and developed an integrated disaster mitigation system (Liu [6]). However, the research about risk assessment is still at an early stage in China (Liu et al.[7]). In 2013, Zhejiang Province did a pilot project in Pinyang country, focusing on the technological system of the refined disaster risk assessment of storm tide in coastal plains. Currently, the system is in the stage of application.

Received 2018-05-07; **Revised** 2019-05-06; **Accepted** 2019-08-15
Foundation item: Zhejiang Science and Technology Plan Project (2015C03003, 2017F30008, 2018F10023)
Biography: CHEN Fu-yuan, M.S., primarily undertaking research on coastal engineering and disaster reduction.
Corresponding author: CHEN Fu-yuan, e-mail: 17018750@qq.com

2 ASSESSMENT METHOD AND REFINED CHARACTERISTICS

2.1 *Assessment method*

The risk of storm surge disaster is a combination of the hazard level of disaster causing factors and the vulnerability of disaster-bearing bodies. The hazard level of disaster causing factors is reflected in submerged range and water depth. It represents the extent of the impact of the disaster. The vulnerability of disaster-bearing bodies is reflected in the importance of ground objects and it represents the sensitivity of ground objects to inundation disasters. Disaster risk can be calculated with $R = H \times V$. R is the total risk, H is the hazard-level of disaster causing factor and V is the vulnerability of disaster-bearing bodies (Wisner et al.[8]).

2.2 *Refined characteristics*

2.2.1 CONSIDERATION OF THE COUPLING OF FLOOD, TIDE AND WAVE

The main factors of submerge disaster in coastal

plains include storm surge, astronomical tide, flood and wave. A combination of these factors is most likely to caused serious disaster (Fang and Shi [9]). Therefore, a hazard-level calculation model must fully consider the coupling situation and simulate the nearshore water level field under the circumstances that storm surge, astronomical tide and flood occur simultaneously. According to wind field, nearshore water depth and embankment form, typhoon waves and overtopping discharge volume are simulated.

2.2.2 CONSIDERATION OF DIKE BREACHING

Because coastal plain terrain is low and flat, dikes are the major engineering measures for tide resistance. Dike breaching has significant impact on the storm surge (Xu et al. [10]). Using the physical model of waves to research damage of standard dikes impacted by wave, the results of research show that the main reason of dike breaching is overtopping discharge volume. A large volume of overtopping can lead to severe damage of dike back slope and collapse of dike body (Zhang et al. [11]). Therefore, the overtopping discharge volume, used as the basis for the judgment and simulation of the dike breaching, is determined by tide level, wave height and dike structure.

2.2.3 REFINEMENT OF GROUND OBJECTS

Refinement of disaster risk assessment can be described from the hazard calculation refinement and disaster-bearing bodies vulnerability assessment refinement. In hazard calculation, terrain conditions are based on topographic maps with a scale of 1:10000, and 1: 2000 to 1: 5000 scale topographic maps are used in sensitive and important areas. The dike, second-line dike, highway, buildings and other resistivity water structures are also considered as the terrain conditions and the minimum mesh size is about 10m. Refining the micro-topography conditions in the calculation area to make the hazard calculation more accurate. In the vulnerability assessment of disaster-bearing bodies, the second-level land classification is the basis. Digital maps such as hydraulic maps, electronic maps, transportation maps are collected, and field survey data is gathered. 3S technology is applied to analyze the spatial location and attributes of major disaster-bearing bodies. This leads to the realization of the refined assessment of the smallest unit with ground objects features (Chen et al.[12]).

3 REFINED ASSESSMENT OF STORM SURGE DISASTER IN PINGYANG COUNTY

As shown in Fig. 1, Pingyang county, a small southern coastal city of Zhejiang, is located between Aojiang river and Feiyun river. Due to its special geographical location, Pingyang is one of the most frequent regions of typhoon disaster in China and is known as the hometown of typhoon disaster.

Figure 1. Location of Pingyang County.

3.1 *Hazard calculation of storm surge*

Storm surge, a common natural catastrophic event, leads to high variation of tidal level caused by the co-existence of astronomic tide and tropical cyclone, both of which are mutually independent events. A tropical cyclone is a storm system characterized by a large low-pressure center and numerous thunderstorms that produce strong winds and heavy rains. The tidal level rises unexpectedly due to the low pressure of tropical cyclone. Strong winds can cause huge wave to impact

coastal dikes and heavy rains lead to floods which rise the water level of estuary. In generally, coastal storm surge disasters are mainly caused by the simultaneous events of cyclone, flooding, high astronomical tide and wave. Therefore, the most unfavorable case for disaster assessment can be designed as the combination of these four factors. Numerical model is used to calculate disaster situation.

3.1.1 NUMERICAL MODEL

Storm surge hazard calculation uses the typhoon-astronomical-flood-wave coupled floodplain numerical model. The refined model has characteristics of high efficiency, accuracy, conservation and automatic capture of intermittent flow. The governing equation is described by shallow water equation.

$$\frac{\partial \eta}{\partial t}+\frac{\partial (hU)}{\partial x}+\frac{\partial (hV)}{\partial y}=0 \tag{3-1}$$

$$\frac{\partial (hU)}{\partial t}+\frac{\partial}{\partial x}(hU^2+\frac{1}{2}gh^2)+\frac{\partial}{\partial y}(hUV)=-gh(S_{ox}-S_{fx}-S_{px})+F_{bx}+\tau_{fiwx} \tag{3-2}$$

$$\frac{\partial (hV)}{\partial t}+\frac{\partial}{\partial x}(hUV)+\frac{\partial}{\partial y}(hV^2+\frac{1}{2}gh^2)=-gh(S_{oy}-S_{fy}-S_{py})+F_{by}+\tau_{fiwy} \tag{3-3}$$

In the equation, η and h are water level and depth. U and V are velocity in x and y direction. S_{ox} and S_{oy} are topographic slope in x and y direction. S_{fx} and S_{fy} are riverbed friction in x and y direction. S_{px} and S_{py} are atmospheric pressure gradient in x and y direction. τ_{fiwx} and τ_{fiwy} are wind drag force in x and y direction.

The calculation of typhoon wind and pressure fields is an important part of storm surge calculation and a decisive factor for storm surge forecast accuracy (Ma et al.[13]). The paper chooses the Jelesnianski (65 type) model for the wind and pressure field (Jelesnianski[14]).

$$W=\begin{cases}\dfrac{r}{r+R}(V_{0x}i+V_{0y}j)+W_R\left(\dfrac{r}{R}\right)^{\frac{3}{2}}(Ai+Bj)/r, & (0<r\leqslant R)\\ \dfrac{R}{r+R}(V_{0x}i+V_{0y}j)+W_R\left(\dfrac{R}{r}\right)^{\beta}(Ai+Bj)/r, & (r>R)\end{cases} \tag{3-4}$$

$$W=\begin{cases}P_0+\dfrac{1}{4}(P_\infty+P_0)\left(\dfrac{r}{R}\right)^3, & (0<r\leqslant R)\\ P_\infty-\dfrac{3}{4}(P_\infty-P_0)\dfrac{R}{r}, & (r>R)\end{cases} \tag{3-5}$$

In the equation, R is maximum wind speed radius, r is distance from the calculated point to the center of the typhoon, $(V_{0x}\ V_{0y})$ is typhoon moving speed, $A=-[(x-x_c)\sin\theta+(y-y_c)\cos\theta]$, and $B=(x-x_c)\cos\theta+(y-y_c)\sin\theta$. $(x\ \ y)$ and $(x_c\ \ y_c)$ are calculated point coordinates and typhoon center coordinates. θ is inflow angel, P_0 is typhoon center pressure, P_∞ is atmospheric pressure at infinity distance and W_R is typhoon maximum wind speed.

Waves caused by typhoon are simulated by SWAM model. The mode can describe the evolution of wave fields under specific wind, flow and underwater terrain conditions in shallow waters. The governing equation is as follows.

$$\frac{\partial}{\partial t}N+\frac{\partial}{\partial x}C_xN+\frac{\partial}{\partial y}C_yN+\frac{\partial}{\partial \sigma}C_\sigma N+\frac{\partial}{\partial \theta}C_\theta N=\frac{S}{\sigma} \tag{3-6}$$

In the equation, N is wave action, σ is relative frequency of waves, θ is wave direction, and S is source item. Cx and Cy are wave propagation speed in x and y direction, respectively. C_σ is propagation speed of wave action in frequency field, and C_θ is the propagation speed of wave action in wave direction field.

Simulation of overtopping and dike-breaching is an important innovation of this model. In the simulation of water flow over dike, according to water level in front of dike, the weir formula is used to calculate flood evolution process. In the simulation of dike-breaching, the varying dike top elevation is applied according to overtopping discharge volume to simulate the process of dike-breaching.

3.1.2 MODEL BUILDING

The model based on the finite volume method with unstructured meshes and the computational domain is divided into a series of triangles and quadrangles. As shown in Fig. 2, the water-level boundary is set close to the first warning line of typhoon, including the Bohai Sea, Yellow Sea, East China Sea, Tamar Channel and Taiwan Strait, etc. Therefore, it can simulate the typhoon evolution. The model's upper discharge boundaries are located at Xuekou station in Feiyun river and Daitou station in Aojiang river. The discharge boundaries accurately describe the flood flow process using measured data. The calculation area accurately depicts the terrain conditions, the dike, high-way and other water-resistivity structures during the mesh generation. The mesh has 575913 units and 292224 nodes, the land grid side length is less than 50m and the minimum grid side length is about 10m. The model is calibrated with the measured data during last 20 representative typhoons. Calibrated parameters include wind field, water level, wave, flood-inundation and so on. The model has been validated to have enough accuracy to simulate flood, storm surge and wave and it can be applied to hazard

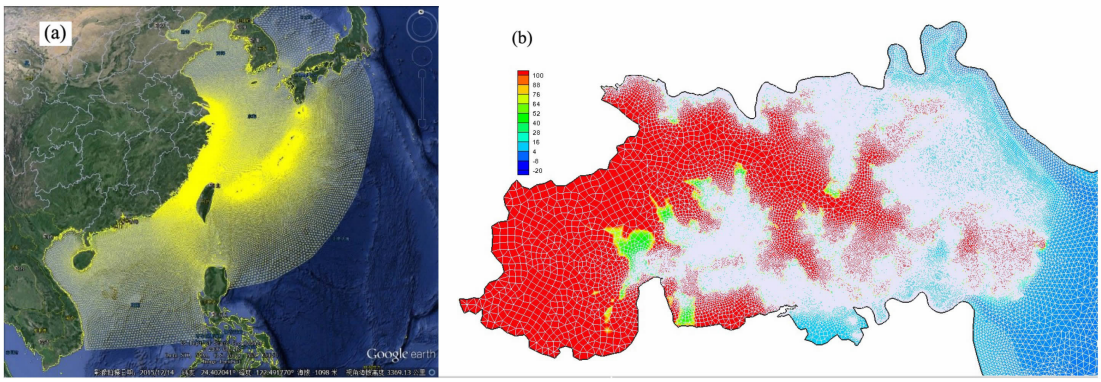

Figure 2. Meshes of model (a) and refined meshes in Pingyang (b).

calculation.

Wave calculation domain uses a rectangular grid and it is gradually refined with five layers of nesting. The first layer grid size is 4000m×4000m and the second layer grid scale is 1000m×1000m, which covers all coastal areas of Zhejiang. The third layer grid scale is 500m×500m and the fourth layer grid size is 300m×300m, which covers Wenzhou. The fifth layer grid scale is 30m×30m, which covers concerned area.

3.1.3 NUMERICAL PARAMETERS

As mentioned above, the hazard of storm surge mainly depends on the parameters of tropical cyclone, astronomic tide, flood and wave.

For tropical cyclone, the meteorological factors include central pressure depression, wind velocity and tracks. According to the risk assessment of storm surge disaster in the USA, typhoon intensity hierarchy can be classified by the central pressure of typhoon and wind speed (Liu et al.[15]). There is a statistical relationship between the central pressure and the wind speed. There are two typical ways to determine typhoon track: the historical experience method and the Monte Carlo method (Chen and Yu[16]). The former is based on the very representative typhoon track in history, while the latter generates a serious of random typhoon tracks based on the Monte Carlo method. Theoretically, the latter with infinite samples is more reasonable than the former (Liu et al.[17]), but it needs very expensive computations (Li et al.[18]), and it is not suitable for practical engineering calculations. It has been proved that the disadvantaged typhoon track determined by the Monte Carlo method is very similar to that determined by the historical experience method (Chen et al.[12]). After the comparison of historical typhoon hazards, the track of Saomei (0608), as shown in Fig. 3, is selected as the representative case in our calculation. Once the typhoon track is determined, the track is moved along the coastal line to find the most disadvantaged case for the concerned area.

In China, most typhoon events occur during the period from June to October, so the average high tidal level of astronomic tide during the typhoon period in the last 20 years is adopted as the representative astronomic tidal level in our calculation. By means of statistical method, the typical tidal process of Pipamen station in which the high tidal level equates the above-mentioned statistical value is selected in the simulation.

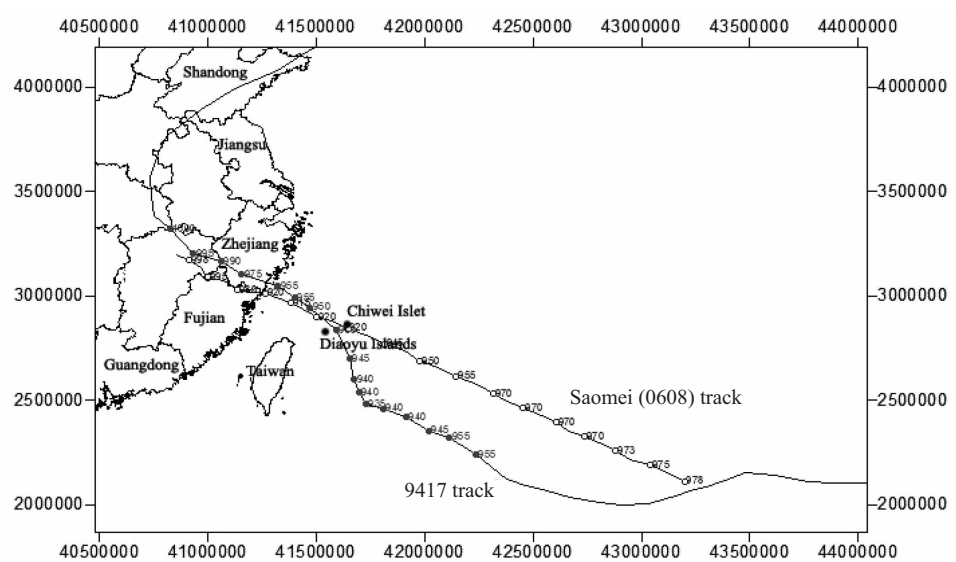

Figure 3. Selection of typhoon path in the simulation.

The flood in Pingyang basin comes from Aojiang river and Feiyun river. Due to different characteristics of two rivers, the property of basin flood is also different. From the historical data analysis, the average flood process of two rivers during the typhoon period is adopted as the discharge boundaries in numerical simulation.

For the low-lying coastal plains, dikes are the most important defense facilities for coastal regions. The location and length of breaching dike are the critical factors of inundation range and depth during the storm surge. Wave caused by typhoon is the main reason of dike-break. Wave overtopping against seawalls is a complicated hydrodynamic phenomenon, and the overtopping discharge volume is one of the most important factors for the safety analysis of dikes. According to the statistical analysis results of physical experiments, the threshold of dike breaching adopted in our calculation is 0.05 $m^3/m \cdot s$.

3.1.4 NUMERICAL RESULTS

Under these aforementioned boundary conditions, the hazard of storm surge for Pingyang is simulated. The submerged range and the distribution of hazard degree during the typhoon event with a central pressure of 945hPa are shown in Fig. 4, in which the hazard degree is determined by the maximum inundation depth.

The hazard class I is distributed mainly in part of Aojiang village, the reclamation area of Wanquan village, and Shuitou village. Hazard class II includes the main part of Aojiang village, Xiaojiang village and part of Wanquan village. Hazard class III includes most part of Kunyang village and part of Wanquan village. Hazard class IV includes part of Kunyang village.

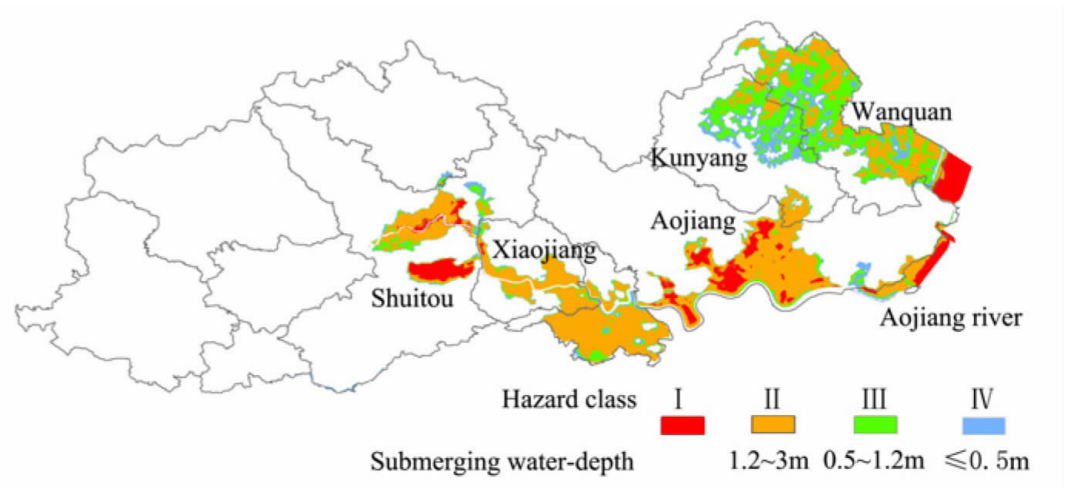

Figure 4. Submerging range at the min-pressure 945pha.

3.2 *Vulnerability assessment of disaster bearing objects*

3.2.1 TERRAIN INFLUENCE

The distribution of inundation scope and maximum water-depth depends on the topographic elevation. Based on an overall analysis of the terrain, astronomical tide, potential storm surge and dike height, the results show that the region with elevation under 7m will be flooded, as shown in Fig. 5.

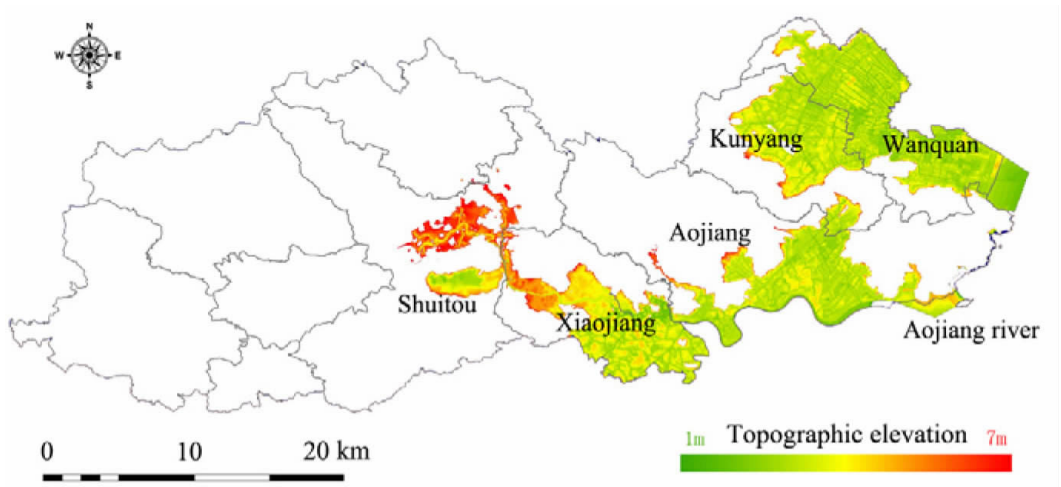

Figure 5. Storm surge vulnerable area.

3.2.2 VULNERABILITY ASSESSMENT METHOD

There are several vulnerability assessment methods, such as the post-disaster evaluation method, social vulnerability concept method, disaster case information method, regional macroeconomic description method, vulnerability curve method (Fan et al.[19]) and so on. All these methods are based on the research on the whole region and the whole region is treated as a unit to analyze the vulnerability, so it is impossible to provide the detailed information for the sub-region. Even though the emphases of these methods are different, the considerations of these methods are within the range of population, houses, economy, infrastructure, public resources, major engineering and so on (Shi et al.[20]). All of these considerations can be represented by the attributes of ground objects. With the development of 3S technique, the digitization of these objects has been achieved and the vulnerability assessment based on ground objects as a unit is viable.

3.2.3 REFINED VULNERABILITY ASSESSMENT

According to their land use, natural and social objects can be classified into 57 categories. Each land use is classified as one of four vulnerability ranks. The vulnerability rank of each category is shown in Table 1 (Zhang et al.[15]).

Table1. Land use classification and vulnerability rank.

Code	Name	Vul rank	Code	Name	Vul rank
011	Rice field	Ⅳ	091	Military facilities	--
012	Irrigated field	Ⅳ	092	Embassy	Ⅰ
013	Dry land	Ⅳ	093	Prison	Ⅰ
021	Orchard	Ⅳ	094	Religion land	Ⅰ
022	Tea plantation	Ⅳ	095	Cemetery	Ⅲ
023	Other plantation	Ⅳ	101	Railway	Ⅱ～Ⅰ
031	Wood land	Ⅳ	102	Highway	Ⅱ
032	Shrub land	Ⅳ	103	Street	Ⅱ～Ⅰ
033	Other wood land	Ⅳ	104	Rural road	Ⅱ
041	Natural pasture	Ⅳ	105	Airport	Ⅱ～Ⅰ
042	Tame pasture	Ⅳ	106	Port	Ⅱ～Ⅰ
043	Other grassland	Ⅳ	107	Pipe transportation	Ⅱ～Ⅰ
051	Wholesale and retail space	Ⅱ～Ⅰ	111	Rivers	Ⅳ
052	Accommodation and catering space	Ⅰ	112	Lakes	Ⅳ
053	Business and finance space	Ⅱ	113	Reservoirs	Ⅳ
054	Other business services space	Ⅱ～Ⅰ	114	Ponds	Ⅳ
061	Industrial land	Ⅱ～Ⅰ	115	Tidal flat	Ⅳ
062	Mining land	Ⅱ～Ⅰ	116	Inland flat	Ⅳ
063	Storage space	Ⅱ～Ⅰ	117	Canals and ditches	Ⅳ
071	Urban residential land	Ⅰ	118	Hydraulic architecture	Ⅲ～Ⅱ
072	Rural homeland	Ⅰ	119	Glacier and permanent snow	Ⅳ
081	Agencies and organizations space	Ⅰ	121	Vacant land	Ⅳ
082	News and publishing space	Ⅱ	122	Agriculture facility	Ⅳ～Ⅲ
083	School	Ⅰ	123	Field ridge	Ⅳ
084	Hospital and charity	Ⅰ	124	Alkaline land	Ⅳ
085	Sports and entertainment	Ⅱ	125	Marshland	Ⅳ
086	Public facilities	Ⅱ～Ⅰ	126	Sand land	Ⅳ
087	Parks and green space	Ⅲ	127	Bare land	Ⅳ
088	Scenic spots	Ⅲ			

Based on land use classification, some important disaster-bearing ground objects are further distinguished, such as residential area, school, hospital, government departments, major enterprises and chemical enterprises (Zhang et al.[21]). The vulnerability of disaster bearing objects is finely assessed. For Pingyang, 889 important disaster-bearing ground objects are distinguished, which are listed in Table 2.

Table 2. Number of refined classification of hazard bearing objects.

	Refined classification of hazard bearing objects	Number
1	Research and education	193
2	Hospital and other medical and health service	61
3	Agencies and organizations	110
4	Business and finance	37
5	Accommodation and catering	46
6	Wholesale and retail	73
7	Other business services	45
8	News and publishing	3
9	Public facilities	32
10	Scenic spots	11
11	Parks and green space	33
12	Sports and entertainment	4
13	Important enterprise	195
14	Petrochemical enterprise	46

3.2.4 RESULTS OF VULNERABILITY ASSESSMENT

The refined vulnerability assessments of disaster bearing objects in Pingyang are shown in Fig. 6. Vulnerability Rank I covers mainly the downtown of the county and the towns. Vulnerability Rank II covers mainly part of urban towns and surrounding areas. Vulnerability Rank III covers mainly suburban and rural areas. Vulnerability Rank IV covers mainly mountainous and coastal beach areas.

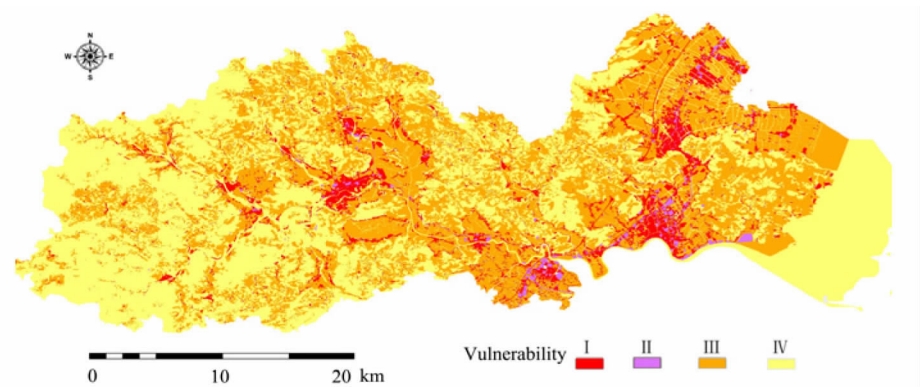

Figure 6. Vulnerability assessment of disaster bearing objects.

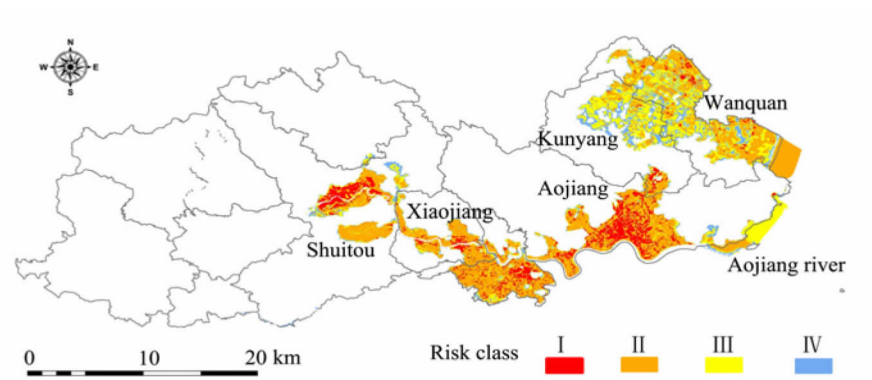

Figure 7. Risk assessment of storm surge disaster.

4 RISK ASSESSMENT OF STORM SURGE DISASTER

Based on the above results of hazard and vulnerability assessment, the risk distribution of storm surge in Pingyang is achieved under the condition of minimum central pressure of 945hPa, as shown in Fig. 7. The risky area from level I to level IV is 25.4 km^2, 91.90

km^2, 48.52 km^2 and 22.36km^2, respectively.

5 CONCLUSION

The refined risk assessment technology of storm surge is realized through the study on hazard factors and disaster bearing bodies. The former accurately simulates the distribution and depth of inundation of storm surge disaster. The latter finely describes the location and attributes of disaster-bearing bodies, which greatly improves the objectivity and practicability of the assessment results. However, other factors such as non-engineering disaster reduction system, public awareness and skills of disaster reduction, pre-alert technology, emergency rescue technology and disaster reduction capabilities (Zhang et al.[22]) are also important factors in reducing the risk of storm surge disasters, although these factors are not considered in this research. In the future, we need to strengthen the research on the effects of the aforementioned factors on the reduction of storm surge disaster risk. Further efforts could be made to realize the comprehensive refinement of storm surge risk assessment.

REFERENCES:

[1] WANG Lu-yang, ZHANG Min, WEN Jia-hong, et al. Flood submergence simulation of composite extreme storms in Shanghai [J]. Adv Water Sci, 2019, 30(4): 1-11 (in Chinese) (online first).

[2] GU Xiao-li, CHEN You-li, QIAN Yan-zhen, et al. Evaluation of typhoon disaster in Ningbo and risk assessment based on analytical hierarchy process [J]. J Trop Meteor, 2018, 34(4): 489-498 (in Chinese).

[3] WANG Hui, LIU Ke-xiu, FAN Wen-jing. Analysis on the sea level anomaly high of 2016 in China coastal area [J]. Acta Oceanol Sinica, 2018, 40(2): 43-52 (in Chinese).

[4] YIN Yi-zhou, HUANG Jian-bin, ZHU Zhi-cun, et al. Analysis on hazards of wind and rain factors associated with tropical cyclones in China's major coastal provinces II: Interdecadal changes [J]. J Trop Meteor, 2018, 34(2): 153-161 (in Chinese).

[5] LI De-lin, XIAO Zi-niu, ZHOU Xiu-hua, et al. Climatic characteristics of abrupt change on tropical cyclone number in the mid-1990s over north western Pacific [J]. J Trop Meteor, 2015, 31(3): 323-332 (in Chinese).

[6] LIU Ming. International experiences of disaster emergency management and its inspiration to China's relevant management [J]. Eco Environ, 2013, (9): 172-175 (in Chinese).

[7] LIU Yian-hua, GE Quan-sheng, WU Wen-xiang. Risk Management-Challenges of New Century [M]. Beijing: China Meteorological Press, 2005 (in Chinese).

[8] WISNER B, BLAIKIE P, CANNON T, et al. At Risk: Natural hazards, people's vulnerability and disasters (Second Edition) [M]. London: Routledge, 2004.

[9] FANG Jia-yi, SHI Pei-jun. A review of coastal flood risk research under global climate change [J]. Progress in Geography, 2019, 38(5): 625-636 (in Chinese).

[10] XU Guo-bin, MENG Qing-lin, YUAN Xi-min. Saline storm surge levee-breach flood numerical simulation and risk analysis [J]. Adv Water Sci, 2016, 27(4): 609-616 (in Chinese).

[11] ZHANG Yao, CHEN Gang, HU Jin-chun. Experimental study on mechanism of sea-dike failure due to wave overtopping [J]. Coastal Engineering, 2017, 36(3): 10-21 (in Chinese).

[12] CHEN Fu-yuan, YUAN Peng, JIN Xin, et al. Vulnerability of flood tide disaster-bearing bodies refined evaluation and classification [J]. Zhejiang Hydrotechnics, 2016, 2: 53-57 (in Chinese).

[13] MA Su-hong, CHEN De-hui. Analysis of performance of regional typhoon model in national meteorological center [J]. J Trop Meteor, 2018, 34 (4): 451-459 (in Chinese).

[14] JELESNIANSKI C P. A numerical calculation of storm tides induced by a tropical storm impinging on a continental shelf [J]. Mon Wea Rev, 1965, 93 (6): 343-358.

[15] LIU Qin-zheng, SHI Xian-wu, GUO Zhi-xing, et al. Guideline for Risk Assessment and Zoning of Storm Surge Disaster[M]. Beijing: State Oceanic Administration, 2015 (in Chinese).

[16] CHEN Fu-yuan, YU Pu-bing. Marine Disaster Risk Assessment and Zoning (Analysis and Application of Random Events Set Selection Method) [R]. Hangzhou: Zhejiang Institute of Hydraulic and Estuary, 2014 (in Chinese).

[17] LIU Yong-ling, FENG Jian-long, FANG Wei-hua. Effects of the tropical cyclone data set length on the result of risk assessment of storm surge [J]. Acta Oceanol Sinica, 2016, 38(3): 60-70 (in Chinese).

[18] LI Ji-hang, GAO Yu-dong, WAN Qi-lin. Sample optimization of ensemble forecast in simulating tropical cyclones based on observed tracks [J]. J Trop Meteor, 2019, 35(4): 197-209 (in Chinese).

[19] FAN Yun-xiao, LUO Yun, CHEN Qing-shou. Research on indexes system about regional vulnerability assessment [J]. Modern Geosci, 2001, 15(1): 113-116 (in Chinese).

[20] SHI Xian-wu, GUO Zhi-xing, ZHANG Yao. A review of research on vulnerability to storm surges [J]. Progress in Geography, 2016, 35(7): 889-896 (in Chinese).

[21] ZHANG Bin, ZHAO Qian-sheng, JIANG Yu-jun. Research on indexes system about regional vulnerability of hazard affected bodies and fine spatial quantitative model [J]. J Catastroph, 2010, 25(2): 36-40 (in Chinese).

[22] ZHANG Xiao-yu, WEI Bo, YANG Hao-yu, et al. Risk assessment of typhoon disaster in Guangdong province based on GIS [J]. J Trop Meteor, 2018, 34 (6): 783-790 (in Chinese).

Citation: CHEN Fu-yuan, YU Pu-bing, WU Xiu-guang, et al. Refined risk assessment of storm surge disaster in coastal plain: A case study of Pingyang county [J]. J Trop Meteor, 2019, 25(3): 304-311.